

## Fermi surface nesting and phonon instabilities in simple cubic calcium

Ion Errea<sup>a,b,\*</sup>, Miguel Martinez-Canales<sup>a,b</sup>, Artem R. Oganov<sup>c,d</sup> and Aitor Bergara<sup>a,b,e</sup>

<sup>a</sup>Materia Kondentsatuaren Fisika Saila, Zientzia eta Teknologia Fakultatea, Euskal Herriko Unibertsitatea, Bilbo, Basque Country, Spain; <sup>b</sup>Donostia International Physics Center (DIPC), Paseo de Manuel Lardizabal, Donostia, Basque Country, Spain; <sup>c</sup>Laboratory of Crystallography, Department of Materials, ETH Zurich, Zurich, Switzerland; <sup>d</sup>Geology Department, Moscow State University, Moscow, Russia; <sup>e</sup>Centro Mixto CSIC-UPV/EHU, Donostia, Basque Country, Spain

(Received 19 June 2008; final version received 21 September 2008)

Phonon instabilities and Fermi surface nesting are studied in the high-pressure simple cubic phase of calcium by means of *ab initio* calculations. We have focused on nesting along  $\Gamma X$ , which could be responsible for some of the anomalies observed in the phonon spectrum. Phonon frequencies calculated with the density functional perturbation theory are imaginary at several Brillouin-zone points (e.g. at  $M$ ). However, including anharmonic contributions to the potential might be crucial to stabilize simple cubic calcium, as solving the Schrödinger equation associated to the transversal unstable mode at  $M$  gives a positive frequency.

**Keywords:** simple cubic calcium; fermi surface nesting; phonon instabilities; anharmonicity; high pressure

### 1. Introduction

As pressure is raised, simple metals undergo a series of structural phase transitions that induce complexity in their electronic properties enhancing superconductivity. Lithium is the clearest example of such features [1–4] since its  $T_c$  is increased by four orders of magnitude at around 40 GPa [5–8]. Among alkaline earth metals, calcium exhibits the most remarkable phase diagram. It is well known that the equilibrium *fcc* phase transforms into *bcc* at 19.5 GPa and into *sc* at 32.0 GPa [9]. The striking reduction in the coordination number as calcium is compressed can be understood via the pressure-induced *s* to *d* electronic transfer [10,11]. Recent experiments [12] have confirmed that the simple cubic phase remains stable up to 109 GPa and further transforms to the still not completely clarified phases Ca-IV at 113 GPa and Ca-V at 139 GPa [13]. This complex behavior is especially reflected in the fact that calcium becomes the element with the largest  $T_c$  among all pressure-induced superconductors. The critical temperature reaches 25 K at 161 GPa in the Ca-V phase [14]. Actually, calcium already superconducts, though at lower temperatures, in

\*Corresponding author. Email: ierrea001@ikasle.ehu.es

the range of pressures where the *sc* phase is stable. However, it is worth noting that the simple cubic phase in calcium presents serious theoretical problems. For instance, linear response calculations revealed that it is mechanically unstable in the corresponding pressure range [15]. In this work we will analyze the effect of Fermi surface nesting as a possible origin of the observed instabilities and the role of anharmonicity in its stability.

This work is divided into four different sections. The computational method is presented in Section 2. Section 3 includes our results and, finally, conclusions are given in Section 4.

## 2. Computational method

Total energies presented in this work have been computed within the density functional theory [16,17] framework, whereas phonon frequencies have been calculated using the density functional perturbation theory (DFPT) [18] as implemented in the Quantum-Espresso (PWscf) package [19]. The exchange correlation functional has been approximated with the Perdew-Burke-Ernzerhof (PBE) parametrization [20], and the core electrons have been modeled with an ultrasoft pseudopotential [21]. It should be noted that the pseudopotential used includes semicore *s* and *p* electrons as well as the *d* shell. Convergence for the plane-wave basis has been achieved with a 70 Ry cutoff for the wave function and 700 Ry for the density. The integration over the Brillouin-zone (BZ) has been performed on a  $28 \times 28 \times 28$  mesh [22] for the *sc* phase, a  $18 \times 18 \times 18$  mesh for the *bcc* phase and a  $16 \times 16 \times 16$  mesh for the *fcc* phase. Phonon dispersion curves have been calculated from the interatomic force constant matrix that has been Fourier interpolated from a  $6 \times 6 \times 6$  grid.

## 3. Results

### 3.1. Phase diagram and phonon instabilities

The enthalpies of the relevant phases (*fcc*, *bcc* and *sc*) of calcium are shown in Figure 1 up to 100 GPa. According to these calculations, the *fcc* to *bcc* transition is predicted at 8.1 GPa whereas the *bcc* to *sc* transition should occur at 39.5 GPa.

Our results slightly differ from the experimental values although they are in good agreement with recent theoretical calculations by Jona and Marcus [23]. The  $T = 0$  calculation performed

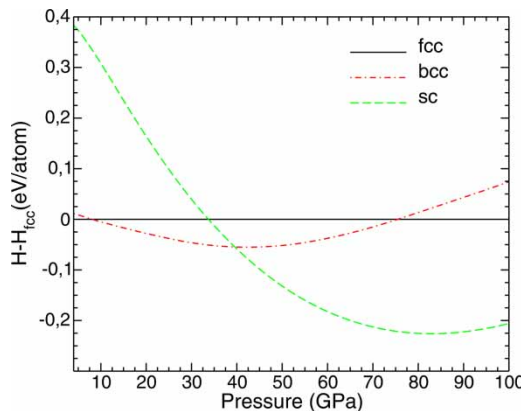


Figure 1. Enthalpy curves comparing *fcc*, *bcc* and *sc* phases of calcium.

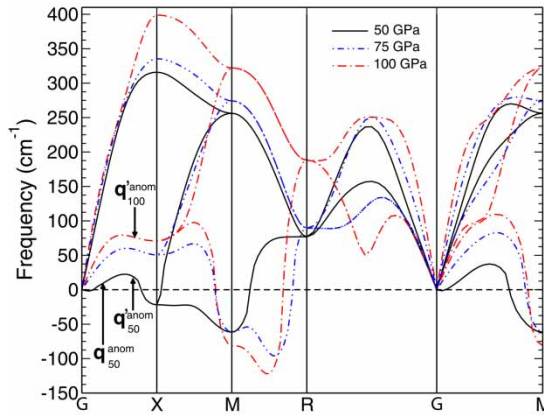


Figure 2. Phonon spectrum of simple cubic calcium at 50, 75 and 100 GPa. At these pressures unstable phonon modes appear at different points of the BZ. Anomaly vectors coming from nesting are depicted in their corresponding positions.

here neglects both the zero-point energy and temperature effects, which might be important to explain this difference.

Focusing on the range of pressures where *sc* is experimentally stable and wondering about its dynamical stability, in Figure 2 we present the DFPT phonon spectrum at 50, 75 and 100 GPa. Interestingly, at 50 GPa the transversal mode shows different unstable ranges along  $\Gamma X$ , both close to  $\Gamma$  and  $X$ . The situation becomes even worse along  $XM$ , where at 50 GPa a complete phonon branch becomes unstable, the strongest instability being at  $M$ . Although at higher pressures phonons close to  $\Gamma$  become stable, transversal modes do not show the usual sinusoidal behavior along  $\Gamma X$ . Even more remarkably, both at 75 and 100 GPa, one of the transverse modes becomes unstable at  $M$ , reaching the strongest instability along  $MR$ .

### 3.2. Fermi surface nesting

As soon as dynamical instability is found contradicting recent experimental results [12], the question of the origin of such instabilities arises. Whether Fermi surface nesting can account for them is an open question. The effect of divergences in the electronic susceptibility on phonon instabilities has been long studied in the literature [24,25], and pressure induced phase transitions in lithium have also been explained via nesting [26,27]. This is an open possibility in calcium. The complexity of the calcium Fermi surface is apparent in Figure 3, where a striking deviation from the quasi-spherical ambient pressure Fermi surface is appreciated [28,29]. Three different bands cross the Fermi energy and its general features are almost unaffected by pressure. Figures 3b and c (Figures 3d and e) shows  $\Gamma XM$  and  $\Gamma MR$  cross sections of the Fermi surface of calcium at 50 GPa (100 GPa). At 50 GPa two nesting momenta are dominant:  $\mathbf{q}_{50}^{\text{nest}}$  and  $\mathbf{q}'_{50}^{\text{nest}}$ . In order to study their effect in the phonon spectrum, in case it extends to the second BZ, we need to fold it back into the first BZ with the addition of a reciprocal lattice vector. Therefore, as  $\mathbf{q}_{50}^{\text{nest}}$  expands out of the first BZ the anomaly corresponding to that nesting is expected at  $\mathbf{q}_{50}^{\text{anom}} = \mathbf{q}_{50}^{\text{nest}} + \mathbf{G}$ , with  $\mathbf{G} = 2\pi/a[-1, 0, 0]$ . Since  $\mathbf{q}'_{50}^{\text{nest}}$  belongs to the first BZ, the phonon instability is expected at the same momentum,  $\mathbf{q}'_{50}^{\text{anom}} = \mathbf{q}'_{50}^{\text{nest}}$ . Figure 3d evidences the main differences in the evolution of the Fermi surface of *sc* calcium under pressure. The bending of the surface at 100 GPa makes one of the nestings rotate to another direction, so that, as it is observed in Figure 3e, only one of the nestings ( $\mathbf{q}'_{100}^{\text{nest}}$ ) remains along  $\Gamma X$ .

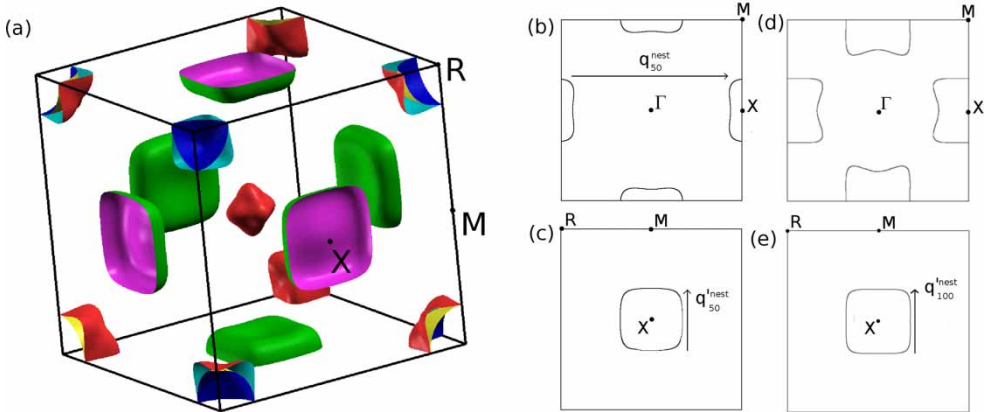


Figure 3. (a) Fermi surface of simple cubic calcium at 50 GPa.  $\Gamma XM$  (b) and  $XMR$  (c) cross sections of the Fermi surface at 50 GPa. Only the band with clear nesting is depicted. Two nesting momenta ( $\mathbf{q}_{50}^{\text{nest}}$  and  $\mathbf{q}'_{50}^{\text{nest}}$ ) along  $\Gamma X$  are identified.  $\Gamma XM$  (d) and  $XMR$  (e) cross sections of the Fermi surface at 100 GPa. Only one of the nestings ( $\mathbf{q}_{100}^{\text{nest}}$ ) remains under pressure.

The three nesting vectors described above point along  $\Gamma X$ , and are depicted in Figure 2. As can be noted, the negative frequency of the transversal mode close to  $\Gamma$  at 50 GPa is related to  $\mathbf{q}_{50}^{\text{anom}}$ . Additionally,  $\mathbf{q}'_{50}^{\text{anom}}$  lies close to the point in which the frequency of the transversal mode starts to drop and  $\mathbf{q}'_{100}^{\text{anom}}$  may also explain the non-sinusoidal behavior of the transversal modes at 100 GPa close to the BZ boundary.

### 3.3. Anharmonic effects

Although nesting could be related to dynamical instabilities in *sc* calcium, recent experimental results [12] have confirmed the stability of *sc* phase from 32 to 109 GPa. Taking into account this contradiction and considering that anharmonic effects are neglected in our DFPT phonon calculation, it is sensible to consider whether anharmonic effects can stabilize this phase. As can be deduced from Figure 2, in the whole pressure range a phonon transverse mode is unstable at  $M$ , and it becomes an interesting point to analyze anharmonic contributions. Therefore, we have studied the influence of anharmonic effects in  $\omega_M^T$  at 75 GPa.

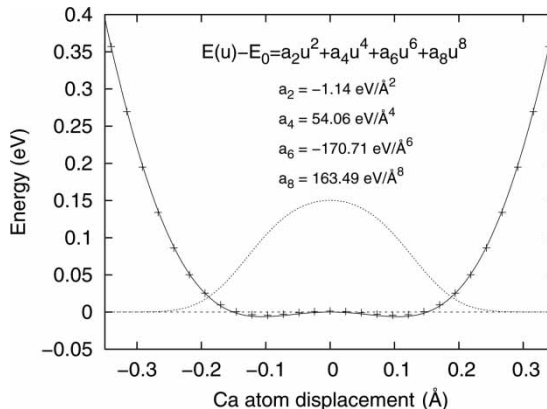


Figure 4. Energy of the supercell containing four atoms of calcium as a function of the atomic displacement according to the transversal unstable mode at  $M$  with 75 GPa. The energy is fitted to an eight-order even polynomial. The squared modulus of the numerically obtained wave function, in arbitrary units, is depicted with a dotted line.

Total energies corresponding to the displacement of atoms according to the transversal mode at  $M$  have been computed using a supercell with four calcium atoms, corresponding to doubling the original cell both along  $x$  and  $y$  directions. The total energy computed as a function of the calcium atom displacement is plotted in Figure 4. As can be appreciated in Figure 4, a very shallow double-well structure, with an approximate depth of 6 meV, is found, and an even polynomial of the eighth order is required to fit the energy accurately. This energy curve is the potential in which the atoms are moving according to the considered transversal mode at  $M$ , and numerically solving its associated Schrödinger equation gives a small but positive frequency,  $\omega_M^T = 23.35 \text{ cm}^{-1}$ . The squared modulus of the numerically obtained wave function shows a broadened maximum when no displacement is considered (see Figure 4). These results confirm the importance of including anharmonic effects in order to stabilize  $sc$  calcium under pressure.

#### 4. Conclusions

This work aims to highlight the importance of nesting in simple cubic calcium and to address the fact that anharmonic effects seem to be crucial for its stability. The nesting vectors studied at 50 and 100 GPa correspond to the instabilities and anomalies observed in the phonon spectrum along  $\Gamma X$ . Additionally, anharmonic contributions are required to stabilize the phonon transversal mode at  $M$ , as solving its associated Schrödinger equation gives a positive frequency, and reveals the importance of including anharmonicity to stabilize the simple cubic phase of calcium. Although being stabilized by anharmonic effects, the question whether simple cubic phase is the real ground state is still unclear and further work is required to unveil the discrepancies between theory and experiment. As was initially predicted for niobium [30] and then for other high-temperature superconductors [31–33], interesting phonon anomalies also arise in many simple elements under high pressure [34–36], where anharmonic effects are crucial to enhance the electron–phonon coupling and considerably increase their associated superconducting transition temperature.

#### Acknowledgements

The research presented herein was performed under project BFM2003-04428, funded by the Spanish Ministry of Education and Science. I.E. would like to thank the Basque Department of Education, Universities and Research for financial help, and M.M.C. is also thankful to the Spanish Ministry of Education and Science for economic support and grant BES-2005-8057. Finally, the authors are also thankful to SGI-IZO SGIker UPV EHU for the allocation of computational resources, as these have made the present work a reality. A.R.O. gratefully acknowledges funding from the Swiss National Science Foundation (grants 200021-111847/1 and 200021-116219) and access to the Skif MSU supercomputer (Moscow State University) and supercomputers at the Swiss Supercomputer Centre (CSCS, Manno).

#### References

- [1] J.B. Neaton and N.W. Ashcroft, *Pairing in dense lithium*, Nature 400 (1999), pp. 141–144.
- [2] A. Bergara, J.B. Neaton, and N.W. Ashcroft, *Pairing,  $\pi$ -bonding, and the role of nonlocality in a dense lithium monolayer*, Phys. Rev. B 62 (2000), pp. 8494–8499.
- [3] A. Rodríguez-Prieto, V.M. Silkin, A. Bergara, and P.M. Echenique, *Anomalous static electronic screening in compressed lithium*, New J. Phys. 10 (2008), p. 053035.
- [4] Y. Ma, A.R. Oganov, and Y. Xie, *High-pressure structures of lithium, potassium, and rubidium predicted by an ab initio evolutionary algorithm*, Phys. Rev. B 78 (2008), p. 014102.
- [5] V.V. Struzhkin, M.I. Erements, W. Gan, H.K. Mao, and R.J. Hemley, *Superconductivity in dense lithium*, Science 298 (2002), pp. 1213–1215.
- [6] K. Shimizu, H. Ishikawa, D. Takao, T. Yagi, and K. Amaya, *Superconductivity in compressed lithium at 20 K*, Nature 419 (2002), pp. 597–599.
- [7] J. Tuoriniemi, K. Juntunen-Nurmilaukas, J. Uusvuori, E. Pentti, A. Salmela, and A. Sebedash, *Superconductivity in lithium below 0.4 millikelvin at ambient pressure*, Nature 447 (2007), pp. 187–189.

- [8] M. Hanfland, K. Syassen, N.E. Christensen, and D.L. Novikov, *New high-pressure phases of lithium*, Nature 408 (2000), pp. 174–178.
- [9] H. Olijnyk and W.B. Holzapfel, *Phase transitions in alkaline earth metals under pressure*, Phys. Lett. 100A (1984), p. 191–194.
- [10] R. Ahuja, O. Eriksson, J.M. Wills, and B. Johansson, *Theoretical confirmation of the high pressure simple cubic phase in calcium*, Phys. Rev. Lett. 75 (1995), pp. 3473–3476.
- [11] H.L. Skriver, *Calculated structural phase transitions in the alkaline Earth metals*, Phys. Rev. Lett. 49 (1982), pp. 1768–1772.
- [12] T. Yabuuchi, Y. Nakamoto, K. Shimizu, and T. Kikegawa, *New high-pressure phase of calcium*, J. Phys. Soc. Jpn. 74 (2005), pp. 2391–2392.
- [13] T. Ishikawa, A. Ichikawa, H. Nagara, M. Geshi, K. Kusakabe, and N. Suzuki, *Theoretical study of the structure of calcium in phases IV and V via ab initio metadynamics simulation*, Phys. Rev. B 77 (2008), p. 020101.
- [14] T. Yabuuchi, T. Matsuoka, Y. Nakamoto, and K. Shimizu, *Superconductivity of Ca exceeding 25 K at megabar pressures*, J. Phys. Soc. Jpn. 75 (2006), p. 083703.
- [15] G. Gao, Y. Xie, T. Cui, Y. Ma, L. Zhang, and G. Zou, *Electronic structures, lattice dynamics, and electron–phonon coupling of simple cubic Ca under pressure*, Solid State Commun. 146 (2008), pp. 181–185.
- [16] P. Hohenberg and W. Kohn, *Inhomogeneous electron gas*, Phys. Rev. 136 (1964), pp. B864–B871.
- [17] W. Kohn and L.J. Sham, *Self-consistent equations including exchange and correlation effects*, Phys. Rev. 140 (1965), pp. A1133–A1138.
- [18] S. Baroni, S. Gironcoli, A. Dal Corso, and P. Giannozzi, *Phonons and related crystal properties from density-functional perturbation theory*, Rev. Mod. Phys. 73 (2001), pp. 515–562.
- [19] S. Baroni, S. de Gironcoli, A. Dal Corso, and P. Giannozzi, <http://www.pwscf.org/>.
- [20] J.P. Perdew, K. Burke, and M. Ernzerhof, *Generalized gradient approximation made simple*, Phys. Rev. Lett. 77 (1996), pp. 1396–1398.
- [21] D. Vanderbilt, *Phys. Soft self-consistent pseudopotentials in a generalized eigenvalue formalism*, Rev. B 41 (1990), pp. 7892–7895.
- [22] H.J. Monkhorst and J.D. Pack, *Special points for Brillouin-zone integrations*, Phys. Rev. B 13 (1976), pp. 5188–5192.
- [23] F. Jona and P.M. Marcus, *Computational study of Ca, Sr and Ba under pressure*, J. Phys. Condens. Matter 18 (2006), pp. 4623–4640.
- [24] W. Kohn, *Image of the Fermi surface in the vibration spectrum of a metal*, Phys. Rev. Lett. 2 (1959), pp. 393–394.
- [25] S.K. Chan and V. Heine, *Spin density wave and soft phonon mode from nesting Fermi surfaces*, J. Phys. F Met. Phys. 3 (1973), pp. 795–809.
- [26] A. Rodriguez-Prieto, A. Bergara, V.M. Silkin, and P.M. Echenique, *Complexity and Fermi surface deformation in compressed lithium*, Phys. Rev. B 74 (2006), p. 172104.
- [27] A. Rodriguez-Prieto, V.M. Silkin, and A. Bergara, *Nesting induced Peierls-type instability for compressed Li-c116*, J. Phys. Soc. Jpn. 76 (2007), pp. 21–22.
- [28] P. Blaha and J. Callaway, *Electronic structure and Fermi surface of calcium*, Phys. Rev. B 32 (1985), pp. 7664–7669.
- [29] C. Lopez-Rios and C.B. Sommers, *Optical properties of calcium*, Phys. Rev. B 12 (1975), pp. 2181–2188.
- [30] W.E. Pickett and P.B. Allen, *Superconductivity and phonon softening. III. Relation between electron bands and phonons in Nb, Mo, and their alloys* Phys. Rev. B 16 (1977), pp. 3127–3132.
- [31] R.E. Cohen, W.E. Pickett, and H. Krakauer, *First-principles phonon calculations for La<sub>2</sub>CuO<sub>4</sub>*, Phys. Rev. Lett. 62 (1989), pp. 831–834.
- [32] J.R. Hardy and J.W. Flocken, *Possible origins of high-T<sub>c</sub> superconductivity*, Phys. Rev. Lett. 60 (1988), pp. 2191–2193.
- [33] R.E. Cohen, W.E. Pickett, and H. Krakauer, *Theoretical determination of strong electron-phonon coupling in YBa<sub>2</sub>Cu<sub>3</sub>O<sub>7</sub>*, Phys. Rev. Lett. 64 (1990), pp. 2575–2578.
- [34] Z.P. Yin, S.Y. Savrasov, and W.E. Pickett, *Linear response study of strong electron-phonon coupling in yttrium under pressure*, Phys. Rev. B 74 (2006), p. 094519.
- [35] D. Kasinathan, J. Kunes, A. Lazicki, H. Rosner, C.S. Yoo, R.T. Scalettar, and W.E. Pickett, *Superconductivity and lattice instability in compressed lithium from Fermi surface hot spots*, Phys. Rev. Lett. 96 (2006), p. 047004.
- [36] O. Degtyareva, M.V. Magnitskaya, J. Kohanoff, G. Profeta, S. Scandolo, M. Hanfland, M.I. McMahon, and E. Gregoryanz, *Competition of charge-density waves and superconductivity in sulfur*, Phys. Rev. Lett. 99 (2007), p. 155505.